SUPPLEMENTARY INFORMATION

Structural analysis of the transitional state of Arp2/3 complex activation by two actin-WCAs

Malgorzata Boczkowska, Grzegorz Rebowski, David J. Kast, Roberto Dominguez

Department of Physiology, Perelman School of Medicine, University of Pennsylvania, Philadelphia, PA 19104

Correspondence should be addressed to R.D. (droberto@mail.med.upenn.edu)

SUPPLEMENTARY FIGURES

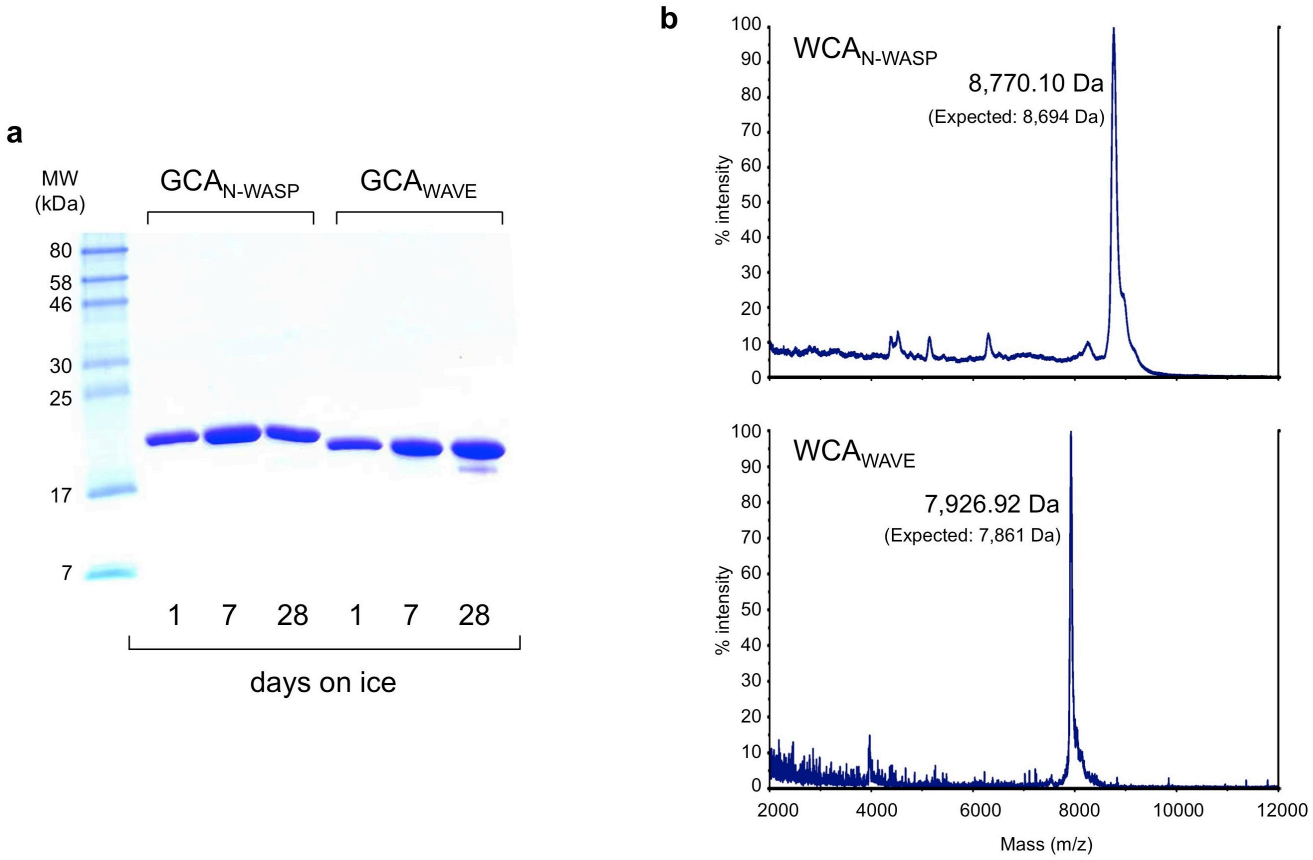

Supplementary Figure S1. Purity and stability of WCA variants. (a) SDS-PAGE analysis of purified $GCA_{N\text{-}WASP}$ and GCA_{WAVE} after 1, 7 and 28 days on ice. (b) MALDI-TOF mass spectrometry analysis of the WCA fragments of N-WASP and WAVE2 stored at -20°C after purification.

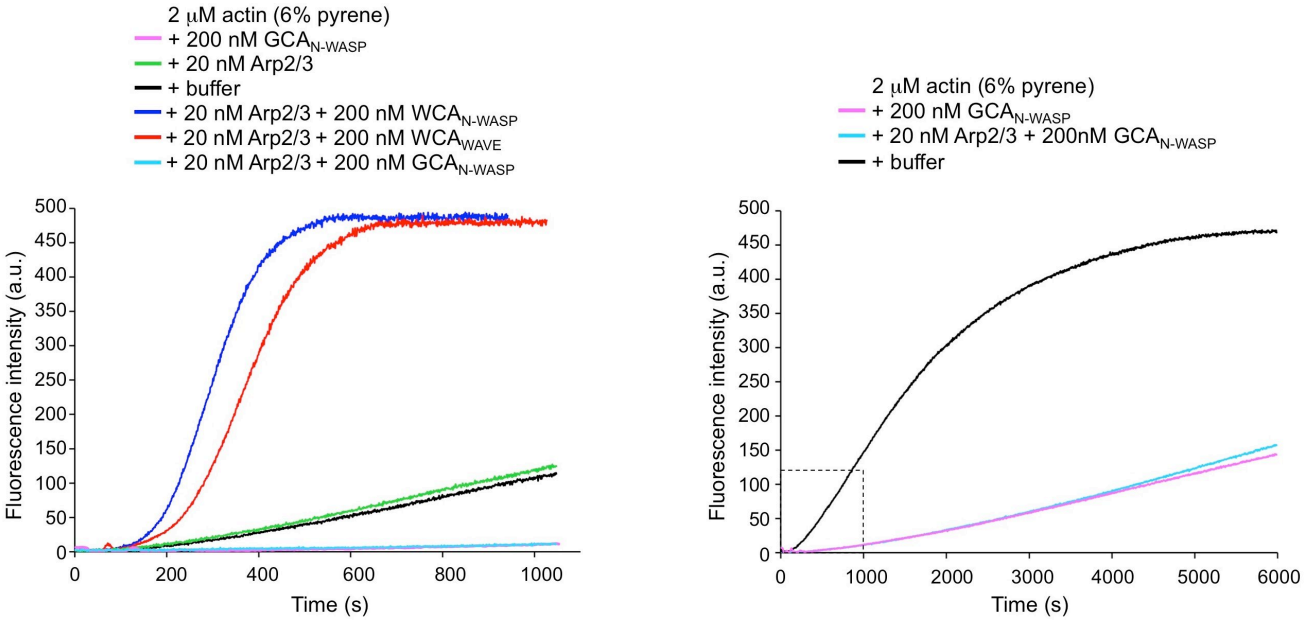

Supplementary Figure S2. $GCA_{N\text{-}WASP}$ inhibits actin polymerization by Arp2/3 complex. Time course of polymerization of 2 μM Mg-ATP-actin (6% pyrene-labeled) alone (black) or in the presence of the indicated proteins (color coded). The graph on the right shows the full time course of spontaneous actin polymerization, whereas that on the left shows the first 1000 s of polymerization (indicated by a dashed box on the right). Actin polymerization was measured as the fluorescence increase resulting from the incorporation of pyrene-labeled actin into filaments, using a Cary Eclipse fluorescence spectrophotometer (Varian). Prior to data acquisition, 2 μM Mg-ATP-actin was mixed with the other reaction components (Arp2/3 complex, $WCA_{N\text{-}WASP}$, WCA_{WAVE}, and $GCA_{N\text{-}WASP}$) in 5 mM Tris pH 7.5, 1 mM $MgCl_2$, 50 mM KCl, 1 mM EGTA, 0.1 mM NaN_3, 0.02 mg ml^{-1} BSA, 0.2 mM ATP. Data acquisition started 10 s after mixing. All the measurements were done at 25°C. Control experiments were carried out with addition of buffer alone.

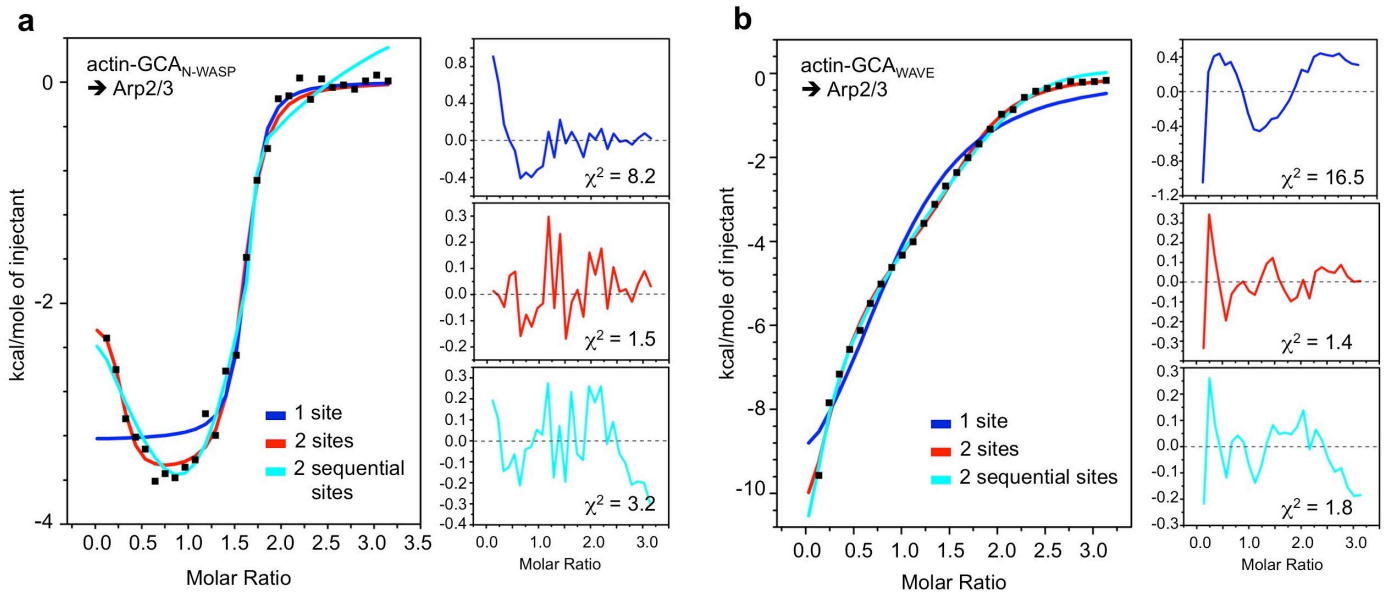

Supplementary Figure S3. Fitting of ITC titration data using different models. (a) The titration of actin-GCA$_{N-WASP}$ into Arp2/3 complex (corresponding to Fig. 2e in main text) fits best to a two-independent-site binding model, as indicated by the residuals and lower χ^2 value of this model. (b) The titration of actin-GCA$_{WAVE}$ into Arp2/3 complex (corresponding to Fig. 4b in main text) also fits best to a two-site binding model.

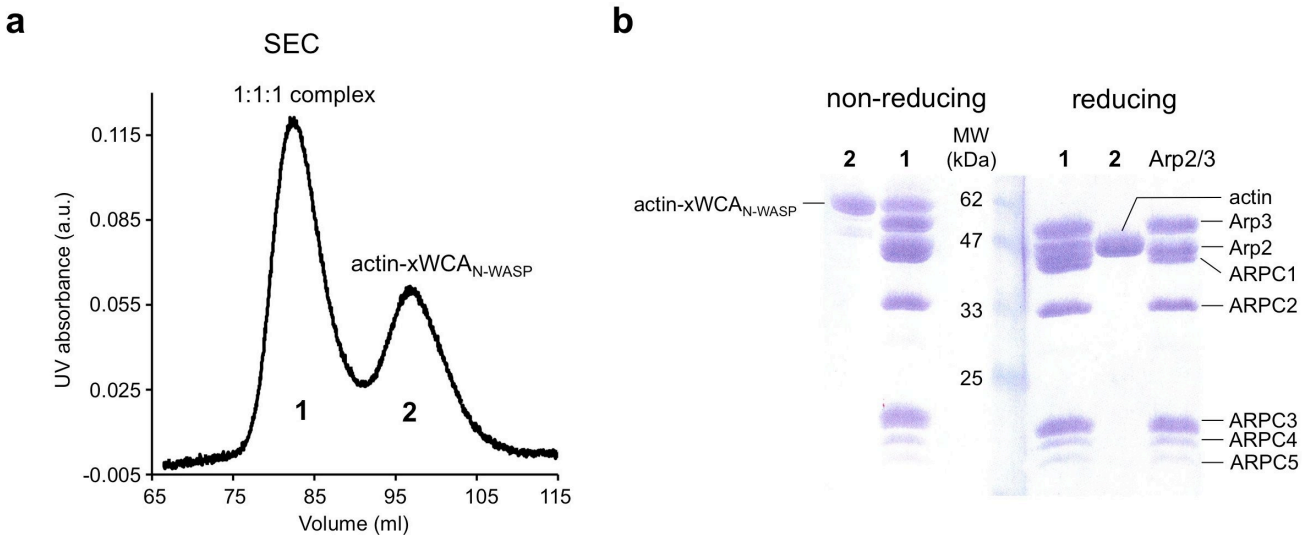

Supplementary Figure S4. Analysis by gel filtration and SDS-PAGE of the saturated 2:2:1 complex of actin-xWCA$_{N-WASP}$-Arp2/3. (a) Purification by gel filtration of the saturated actin-xWCA$_{N-WASP}$-Arp2/3 complex resulting from the experiment shown in figure 2b (main text) results in two well-separated species. (b) Analysis by SDS-PAGE of peaks 1 and 2 under reducing (with addition of 10 mM β-mercaptoethanol) and non-reducing conditions. Peak-1 consists of a 1:1:1 actin-xWCA$_{N-WASP}$-Arp2/3 complex, whereas peak-2 corresponds to actin-xWCA$_{N-WASP}$ dissociating from the weaker affinity site-2. Under non-reducing conditions, actin-xWCA$_{N-WASP}$ remains as a complex. Under reducing conditions, actin and xWCA$_{N-WASP}$ separate, but only actin is observed in the gel since the xWCA$_{N-WASP}$ fragment with molecular mass 8.7 kDa migrates too fast to be observed.

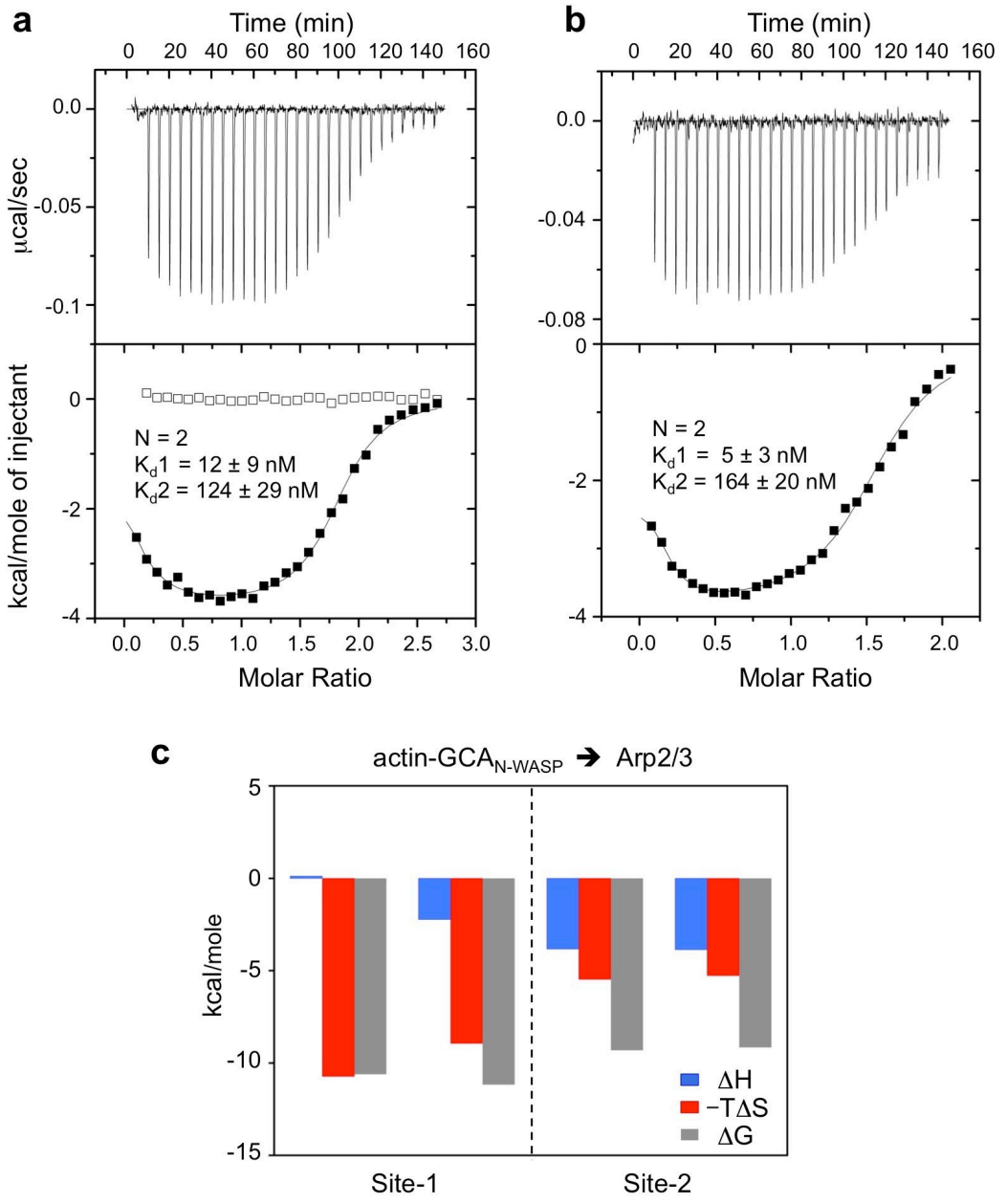

Supplementary Figure S5. ITC titrations and binding isotherms of actin-GCA$_{N\text{-}WASP}$ into Arp2/3 complex. (a) Titration of 73 μM actin-GCA$_{N\text{-}WASP}$ into 5.8 μM Arp2/3 complex. Open symbols correspond to a control experiment in which buffer was titrated into 5.8 μM Arp2/3 complex. (b) Titration of 46 μM actin-GCA$_{N\text{-}WASP}$ into 4.8 μM Arp2/3 complex. These experiments are repetitions of the experiment shown in figure 2e (main text), using lower protein concentrations. Both experiments fit best to two-site binding isotherms. (c) Comparison of the thermodynamic parameters of the titrations.

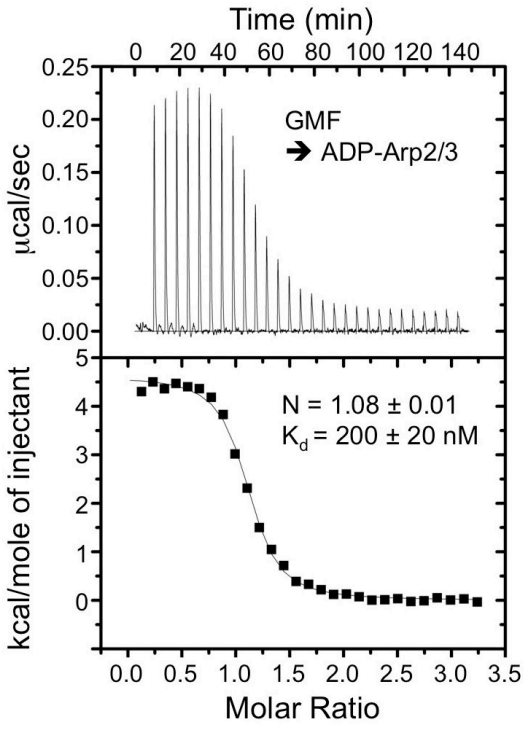

Supplementary Figure S6. Binding of GMF to ADP-Arp2/3 complex. ITC titration of 140 μM GMF into 9.2 μM ADP-Arp2/3 complex. The data fits best to one-site binding isotherm.

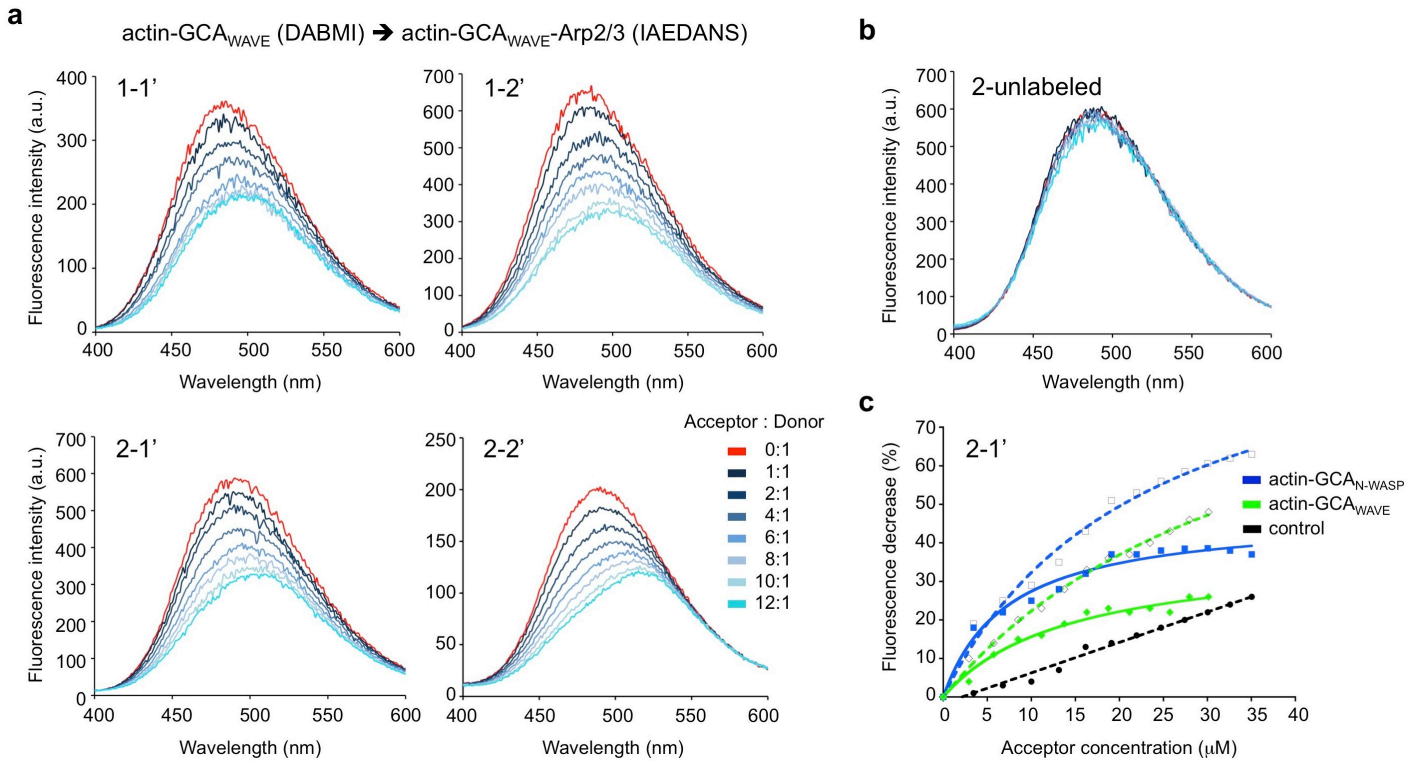

Supplementary Figure S7. Steady state FRET analysis of actin-GCA binding to Arp2/3 complex. (a) Fluorescence quenching during titration of acceptor-labeled actin-GCA$_{WAVE}$ into donor-labeled 1:1:1 actin-GCA$_{WAVE}$-Arp2/3 complex. Probe sites and titration ratios are indicated. (b) Titration of unlabeled actin-GCA$_{WAVE}$ into IAEDANS-labeled actin-GCA$_{WAVE}$-Arp2/3 complex. (c) Decrease in donor peak fluorescence as a function of acceptor concentration for probe positions 2-1' (shown in part a and Fig. 6a of the main text, broken green and blue lines, respectively). The donor peak fluorescence was calculated as the average fluorescence from three independent measurements in the range 480-490 nm. The black broken line represents a control experiment in which DABMI-labeled GCA$_{N-WASP}$ was titrated into IAEDANS-labeled GCA$_{N-WASP}$. The steady-state FRET (solid green and blue lines) was calculated by subtracting the fluorescence decrease observed in the control experiment (black broken line) from the decrease in donor peak fluorescence (broken green and blue lines).

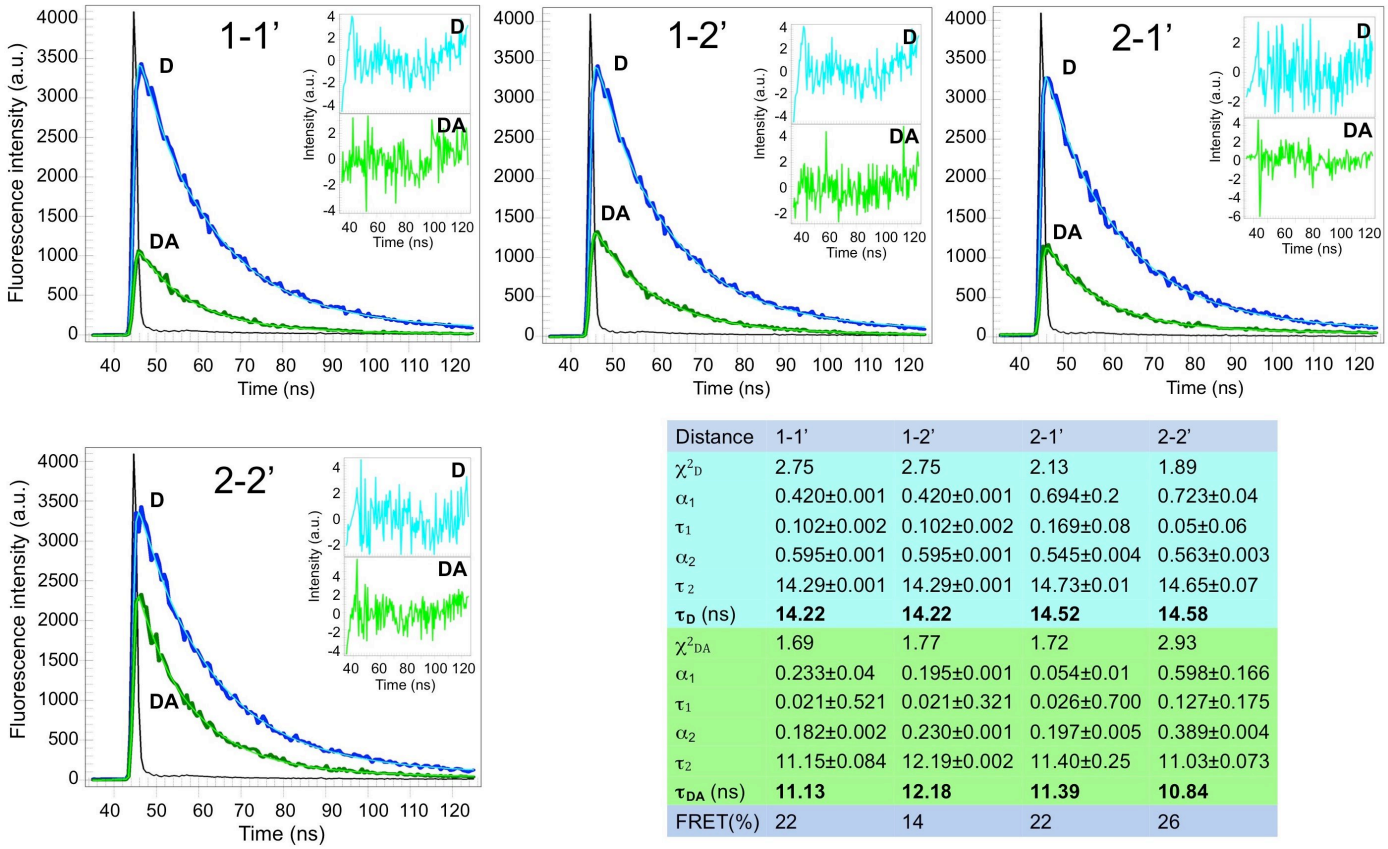

Distance	1-1'	1-2'	2-1'	2-2'
χ^2_D	2.75	2.75	2.13	1.89
α_1	0.420±0.001	0.420±0.001	0.694±0.2	0.723±0.04
τ_1	0.102±0.002	0.102±0.002	0.169±0.08	0.05±0.06
α_2	0.595±0.001	0.595±0.001	0.545±0.004	0.563±0.003
τ_2	14.29±0.001	14.29±0.001	14.73±0.01	14.65±0.07
τ_D (ns)	**14.22**	**14.22**	**14.52**	**14.58**
χ^2_{DA}	1.69	1.77	1.72	2.93
α_1	0.233±0.04	0.195±0.001	0.054±0.01	0.598±0.166
τ_1	0.021±0.521	0.021±0.321	0.026±0.700	0.127±0.175
α_2	0.182±0.002	0.230±0.001	0.197±0.005	0.389±0.004
τ_2	11.15±0.084	12.19±0.002	11.40±0.25	11.03±0.073
τ_{DA} (ns)	**11.13**	**12.18**	**11.39**	**10.84**
FRET(%)	22	14	22	26

Supplementary Figure S8. TR-FRET experiments and data fitting. For each experiment, actin-GCA$_{N\text{-}WASP}$-Arp2/3 complex (300 ml at 5 μM) labeled with the donor probe at position 1 or 2, was pre-purified (as shown in Fig. 2f, main text) and mixed with actin-GCA$_{N\text{-}WASP}$ (at 12-fold molar excess) containing the acceptor probe at position 1' or 2'. The fluorescence decay of donor-only (blue curves) and donor-acceptor (green curves) were recorded for each combination of probe positions (as indicated). The decay data were fitted using a double exponential function (thin traces). The residuals are reported in insets. A color-coded table lists the parameters of the double-exponential fitting of the decay data and calculated average lifetimes (see Methods).

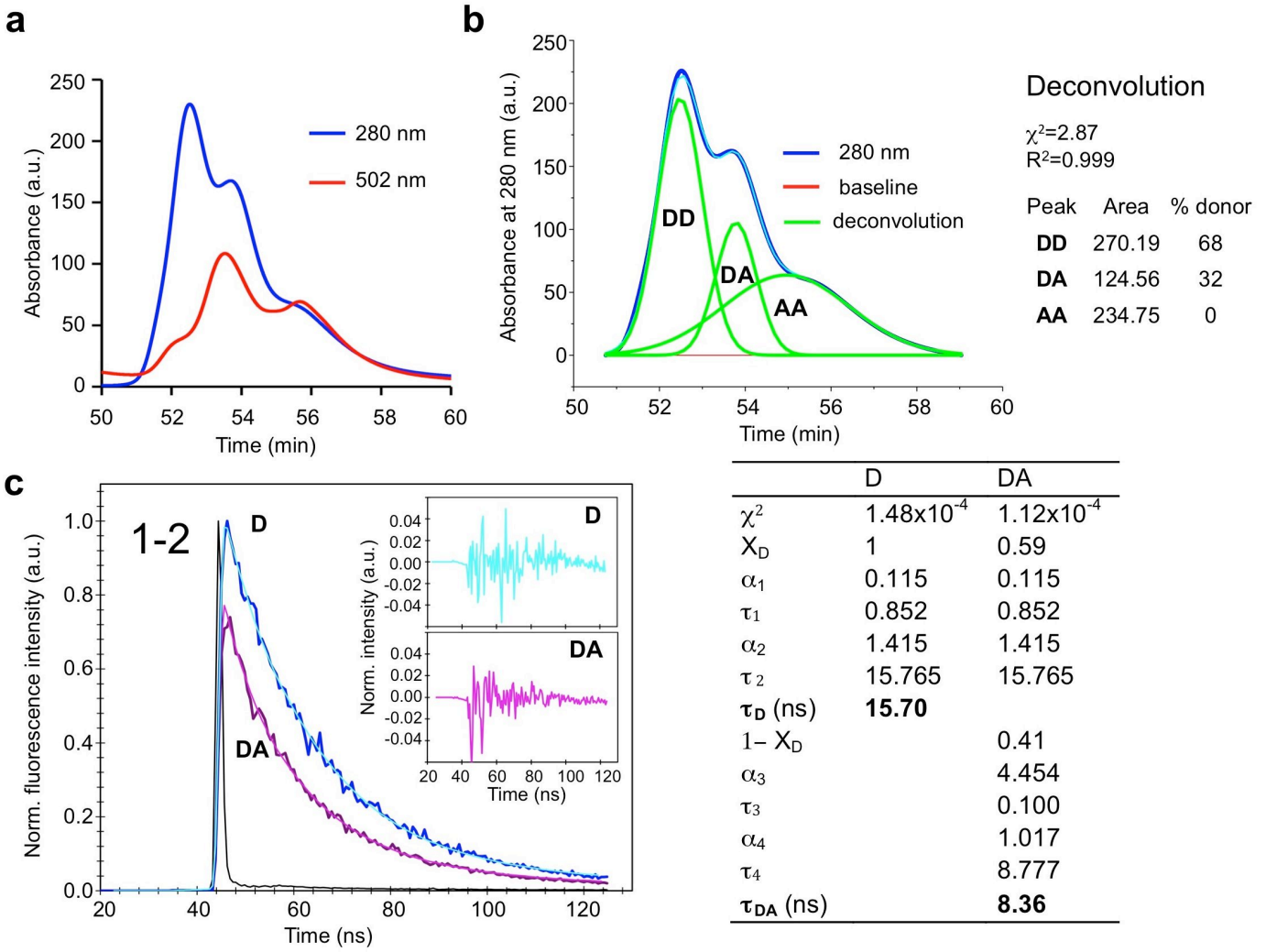

	D	DA
χ^2	1.48×10^{-4}	1.12×10^{-4}
X_D	1	0.59
α_1	0.115	0.115
τ_1	0.852	0.852
α_2	1.415	1.415
τ_2	15.765	15.765
τ_D (ns)	**15.70**	
$1 - X_D$		0.41
α_3		4.454
τ_3		0.100
α_4		1.017
τ_4		8.777
τ_{DA} (ns)		**8.36**

Supplementary Figure S9. TR-FRET experiment with double-labeled $GCA_{N\text{-}WASP}$ bound at site-1. (a) Analysis of double-labeled $GCA_{N\text{-}WASP}$ by HPLC using a reverse-phase C18 column. The protein absorbance spectrum recorded at 280 nm (blue) contains three peaks. The spectrum collected at 502 nm (red) reveals the presence of the DABMI probe in the last two peaks, whereas the fluorescence emission spectra of protein fractions (λ_{ex} = 337 nm, λ_{em} = 400–600 nm) revealed the presence of IAEDANS in the first two peaks (not shown). (b) Deconvolution of the protein spectrum shown in part a (blue) into three species (green) using the Gausssian algorithm of the program Origin. In the fractions in the donor-donor (DD) and acceptor-acceptor (AA) peaks, both cysteines are labeled with a single fluorophore (IAEDANS or DABMI), whereas the fraction in the donor- acceptor (DA) peak is double-labeled with both fluorophores. The area under each peak defines its contribution to the total absorbance spectrum. However, only two fractions, DD and DA, contribute to the fluorescence spectrum, such that their relative contributions are 68% and 32%, respectively. (c) TR-FRET experiment and data fitting. The fluorescence decay of donor-only (blue curve) and donor-acceptor (magenta curve) were corrected for concentration and normalized. The donor-acceptor decay was fitted using a four-exponential function (thin traces), by fixing the values of two of the exponentials according to the double-exponential analysis of the donor-only decay (as in Supplementary Fig. S8). The residuals are reported in insets. The table lists the parameters of the fitting.

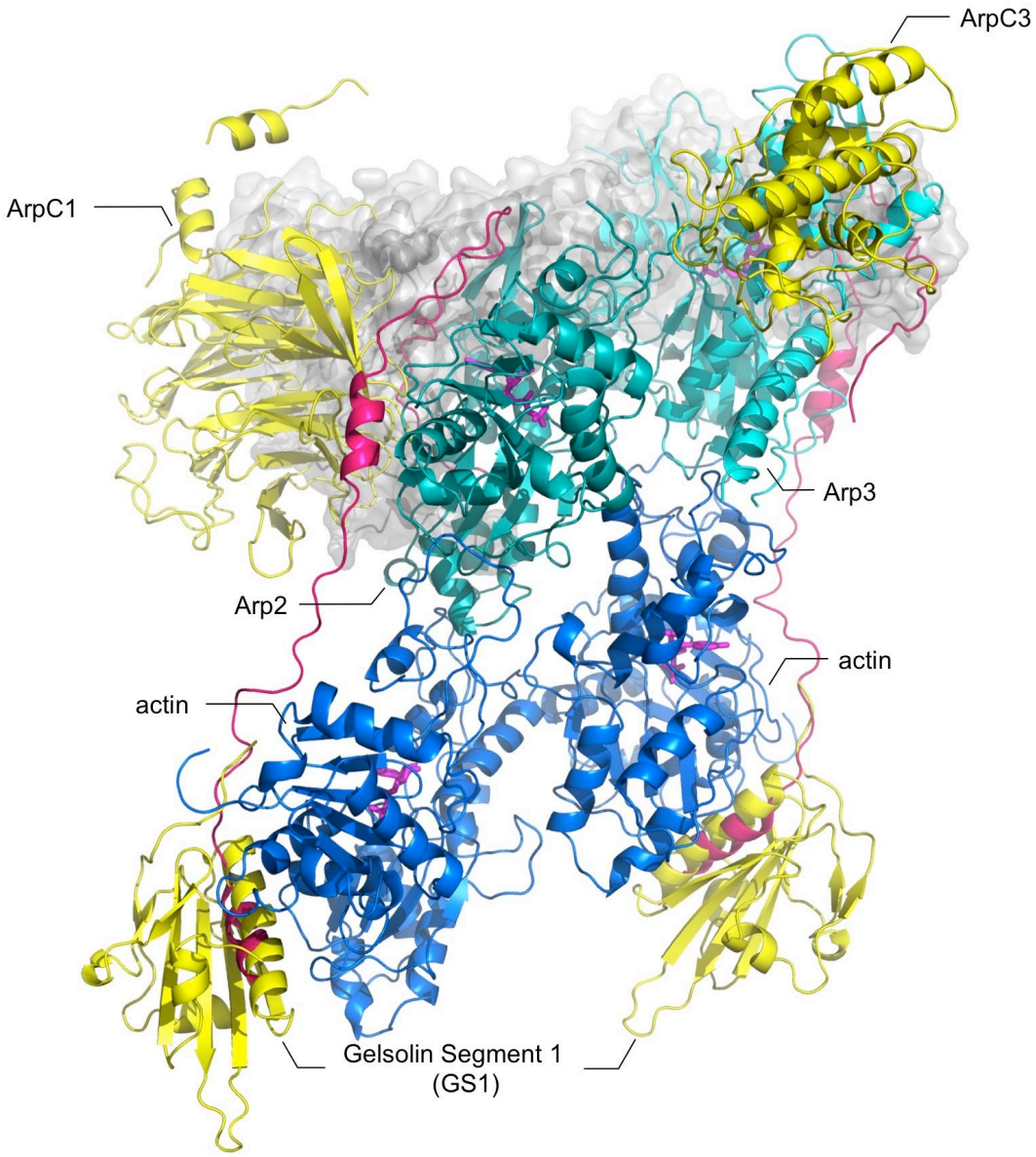

Supplementary Figure S10. The use of GS1 in GCA constructs should not obstruct native interactions within the transitional complex. GS1 in GCA constructs replaces the N-terminal region of the W domain in WCA (see also Fig. 1a in main text), which binds at the barbed end of the first two actin subunits. Note that the GS1 moieties of the two GCA molecules bound to Arp2/3 complex are not expected to interfere with interactions between either the actins or the actins and Arp2/3 complex.

Supplementary Table S1. Thermodynamic parameters of ITC titrations

Ligand (syringe)	Complex (cell)	Site-1			Site-2		
		K_d nM	ΔH kcal/mol	ΔS cal/molK	K_d nM	ΔH kcal/mol	ΔS cal/molK
$WCA_{N\text{-}WASP}$	Arp2/3	20±10	-12.1±3.7	-5.4	182±53	-5.0 ±0.4	13.9
actin-x$WCA_{N\text{-}WASP}$	Arp2/3	3 ± 3	-2.1±0.4	31.8	173±72	-3.8±0.1	18.3
actin-x$WCA_{N\text{-}WASP}$	1:1:1	Saturated			290±61	-3.8±0.2	17.1
actin-x$W_{N\text{-}WASP}$	1:1:1	Saturated			No binding		
actin-$GCA_{N\text{-}WASP}$	Arp2/3	3 ± 2	-2.1±0.3	32.0	123±27	-3.7±0.1	19.3
actin-$GCA_{N\text{-}WASP}$	1:1:1	Saturated			270±25	-5.0±0.1	13.2
actin-GS1	1:1:1	Saturated			No binding		
WCA_{WAVE}	Arp2/3	42±24	-11.0±1.4	-3.2	1050±253	-5.3±0.5	9.7
actin-GCA_{WAVE}	Arp2/3	149±73	-18.2±12.1	-29.9	752±200	-3.9±1.1	15.0
actin-GCA_{WAVE}	1:1:1	205±30	-10.8±0.9	-5.7	1210±274	-5.2±0.3	9.8
GMF	ADP-Arp2/3	200±20	4.6±0.1	46.6			
actin-$GCA_{N\text{-}WASP}$	ADP-Arp2/3	2 ± 1	-15.6±2.3	-13.2	109±25	-2.3±0.1	24.2
actin-$GCA_{N\text{-}WASP}$	GMF-ADP-Arp2/3	92±40	-9.0±2.5	1.4	274±183	-0.6±0.6	28.1

Supplementary Table S2. Primers

Construct	Forward	Reverse
$WCA_{N\text{-}WASP}$	5’ atccatatgtcctgctcaggaagggatgc	5’ acagaattcttagtcttcccactcatcatcatcctc
$xWCA_{N\text{-}WASP}$	5’ atccatatgtgctcctcaggaagggatgcgcttttagac	5’ acagaattcttagtcttcccactcatcatcatcctc
WCA_{WAVE}	5’ atccatatgagtgacgcgcgcagtgacctgctt	5’ acagaattcttaatccgaccagtcgtc
$GCA_{N\text{-}WASP}$	5’ ctgaatccatatggtggtggaacaccccgagttcctc 5’ caagcatgtggctgatggccaagagt	5’ gccacatgcttgaatcctgatgccacac 5’ acagaattcttagtcttcccactcatcatcatcctc
$GCA_{N\text{-}WASP}$ H479C	5’ cagaaaaggagcaaagccatttgttcttcagatgaagatgaaga	5’ tcttcatcttcatctgaagaacaaatggctttgctccttttctg
$GCA_{N\text{-}WASP}$ C502	5’ ctgaatccatatggtggtggaacaccccgagttcctc	5’ cagaattcttaacagtcttcccactcatcatcatcctc
GCA_{WAVE}	5’ ctgaatccatatggtggtggaacaccccgagttcctc 5’ caagcatgttgaagagcaacgg	5’ tcaacatgcttgaatcctgatgccacac 5’ acagaattcttaatccgaccagtcgtc
GCA_{WAVE} E479C	5’ cccgtcggatcgctgtttgttacagcgactcggaagatg	5’ catcttccgagtcgctgtaacaaacagcgatccgacggg
GCA_{WAVE} C498	5’ ctgaatccatatggtggtggaacaccccgagttcctc	5’ acagaattcttaacaatccgaccagtcgtcttcatcaaa
GS1	5’ actgaatccatatggtggtggaacaccccgagttcctc	5’ acagaattcttacacgtgcttgaatcctgatgcc

Supplementary Movie S1. Model of the transitional complex formed by Arp2/3 complex and two actin-WCAs. The movie illustrates the different steps of model building and activation, including the rotation of Arp2 and the pseudo-symmetric binding of WCA molecules constrained by TR-FRET distances.